ARCHIVES OF ACOUSTICS
35, 4, 653–660 (2010)
DOI: 10.2478/v10168-010-0049-6

Technical Note

Annular Array Transducer and Matched Amplifier for Therapeutic Ultrasound

Wojciech SECOMSKI, Andrzej NOWICKI, Janusz WÓJCIK,
Marcin LEWANDOWSKI, Mateusz WALCZAK, Ryszard TYMKIEWICZ

Institute of Fundamental Technological Research
Department of Ultrasound
Polish Academy of Sciences
Pawińskiego 5B, 02-106 Warszawa, Poland
e-mail: Wojciech.Secomski@ippt.gov.pl

(*received November 4, 2010; accepted November 26, 2010*)

The use of therapeutic ultrasound continues to grow. A focused ultrasonic wave can increase the tissue temperature locally for the non-invasive cancer treatment or other medical applications. The authors have designed a seven-element annular array transducer operating at 2.4 MHz. Each element was excited by sine burst supplied by a linear amplifier and FPGA control circuits. The acoustic field, generated by a transducer was initially numerically simulated in a computer and next compared to water tank hydrophone measurements performed at 20, 40 and 60 mm focal depth. The results showed good agreement of the measurements with theory and the possibility to focus the ultrasound in the preselected area. The total acoustic power radiated by the annular array was equal to 2.4 W.

Keywords: ultrasonic therapy, annular array transducer, ultrasonic field.

1. Introduction

Therapeutic ultrasound has been used for many years (Haar, 2008). A focused ultrasonic wave can increase the tissue temperature locally for the non-invasive cancer treatments or healing of the soft tissue injured during sport (Haar, 1999). More recently, high intensity focused ultrasound beams (HIFU) were used for thermal ablation of selected regions. Also low intensity focused ultrasounds (LIFU) were able to stimulate physiological processes such as a tissue repair (Haar, 1999) or increase the blood vessels permeability without any histological damage (Shuto, 2006) or heat responsive gene therapy (Gambin, 2009). In the low intensity (LIFU) applications, the maximum tissue temperature

must not exceed 43°C. This limits the acoustical power to approximately 2 W and depends on the ultrasonic attenuation in the tissue (Wójcik, 1999).

Ultrasonic therapy requires precise positioning of the transducer. The acoustical focus should be placed at a selected tissue area. Different skin to the focal zone distance requires either a set of different focal length transducers or an electronically focused transducer. This is possible with a multi element annular array transducer and electronically steerable delays of signals exciting different annular rings (Arditi, 1982).

2. Materials

The annular array transducer was designed and built on the 20 mm diameter and a 2.0 MHz resonance frequency Pz26 piezoceramic disc. The the back surface of the disc was divided into seven rings of equal area with 100 μm gaps between adjacent rings. The disc was fixed in a metal case and the matching layer was deposited at its front surface. The resonance frequency was changed to 2.4 MHz. The designed transducer and radii of the rings are presented in Fig. 1.

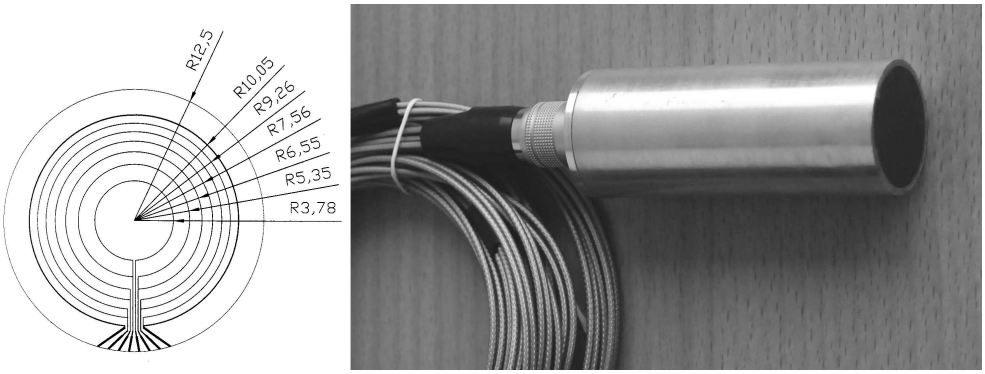

Fig. 1. Radii of the rings and the image of the designed seven-element annular array transducer. The external ring R12,5 is a passive element.

The transmitter consists of seven power amplifiers and seven D/A converters. The 14 bit, 80 MHz AD9717 converters were controlled by the Altera Aria GX FPGA circuit. To minimize harmonics, transducer was excited by a sine wave signal in the form of a 10 period burst and 40 period delay between the bursts (1/5 duty cycle). Such a high duty cycle required modifications of the power amplifier stages. The first stage was a high-speed operational amplifier driving a complementary pair of VMOS transistors in the second stage. The power supply of the second stage was programmed and depended on the required output power. A simplified schematic diagram of the power amplifier is presented in Fig. 2.

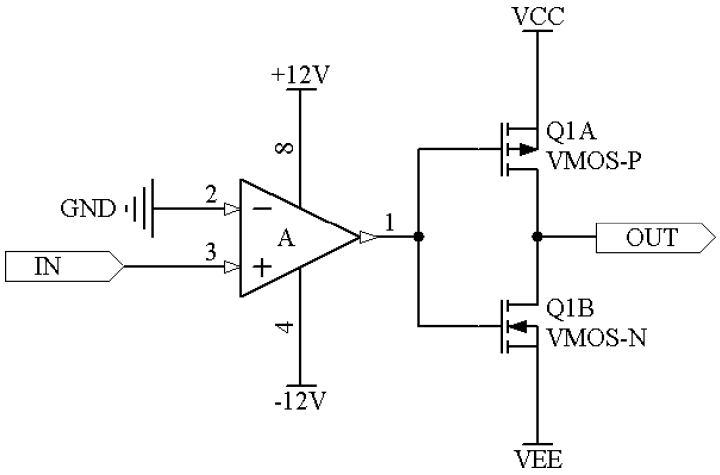

Fig. 2. Simplified schematic diagram of the power stage controlling single element of the transducer. VEE = −VCC.

3. Measurements

First, the admittance of each element was measured. Both the real (conductance) and imaginary (susceptance) parts were measured using a 4395A Impedance Analyzer (Agilent, USA).

Later, the acoustical field generated by the transducer has been recorded using the Isel C142-4 3axix stepper motor scanner (Isel, Germany). The acoustical pressure was measured by the PVDF bilaminar hydrophone S5-259 (Sonora, USA). The hydrophone signal was amplified by the BR-640 broadband receiver (Ritec, USA), and stored in the HP54503A digital oscilloscope (Hewlett-Packard, USA). The acoustic field was scanned at a 10–80 mm distance from the transducer with 1 mm axial and 0.2 mm lateral resolution. The transducer was electronically focused by FPGA circuits at 20, 40 and 60 mm depths. The measured acoustical field was compared to the computer simulations for the 20 mm diameter and 7 element annular array transducer with the same excitation delays between elements. In order to model the propagation of ultrasonic pulses radiated in the attenuating media by acoustic sources, it was necessary to take into account diffraction, thermo-viscous absorption and non-linear effects that may be significant if the source drive levels are high enough (Wójcik, 2008).

Finally, the acoustical power generated by te annular array was measured by the ultrasound power meter UPM-DT-1E (Ohmic Instruments, USA). The transducer was excited by a 10 period of sine wave plus a 40 period delay = 1/5 duty factor. The output power was changed by the amplifier input amplitude. For each measurement, the power supply of the transmitter was adjusted to obtain a not distorted sine wave signal on the transducer and a maximum amplifier efficiency. Power amplifier was tested within ±20 V and ±30 V DC voltage ranges.

4. Results

Results of the admitance measurements are presented in Fig. 3. The peak value of the conductance corresponds to the resonance frequency.

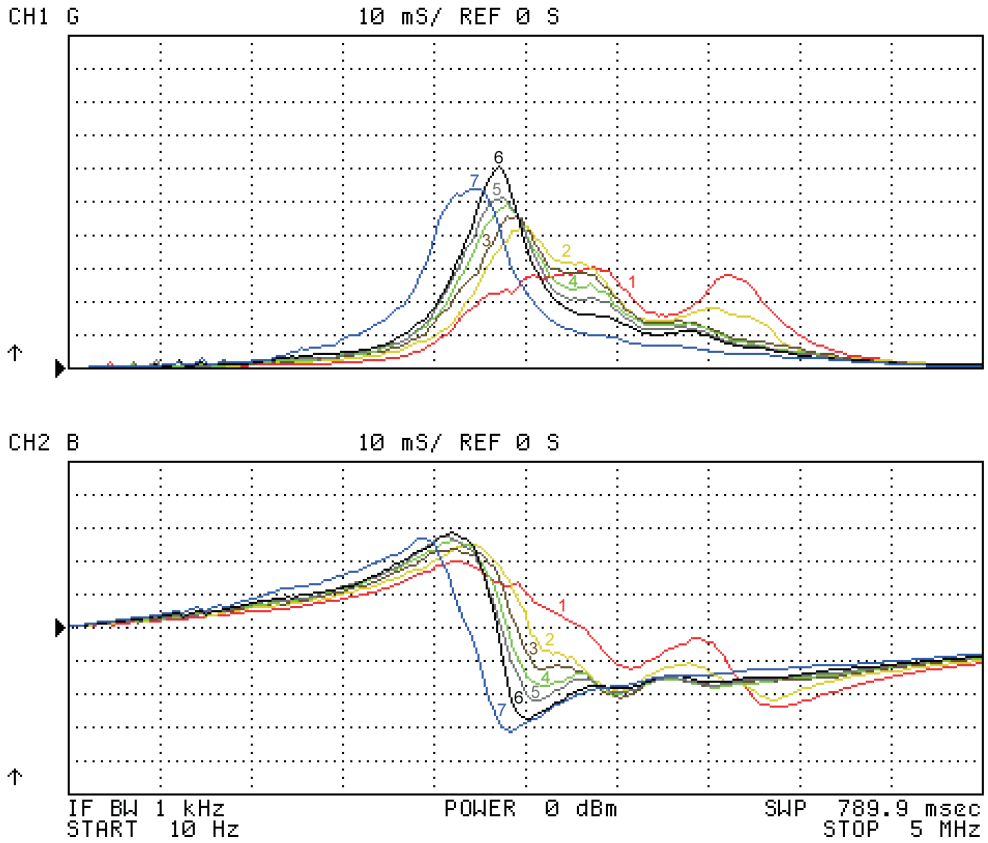

Fig. 3. Admitance of the designed transducer. Real part (top) and imaginary part (bottom). The admitances of separate elements are marked from 1 (central disc) to 7 (external ring). The vertical scale is 10 mS/div and the horizontal one is 500 kHz/div with 2.5 MHz at center.

The on axis pressure distributions, measured and simulated, are presented in Fig. 4. Three measurements for three focal lengths were performed. The results of the acoustical field measurements and computer simulations are presented in Figs. 5–7 at 20, 40 and 60 mm focal depths. For 20 mm, the physical focus was at the $f = 19$ mm distance, the positive peak acoustical pressure at focus was $P_M = 0.66$ MPa and the spatial peak pulse averaged acoustical intensity was $I_{\mathrm{SPPA}} = 14$ W/cm^2. For 40 mm measurements, the corresponding values were $f = 35$ mm, $P_M = 0.72$ MPa and $I_{\mathrm{SPPA}} = 11$ W/cm^2. Finally, for the 60 mm focal depth, the values were $f = 46$ mm, $P_M = 0.57$ MPa and $I_{\mathrm{SPPA}} = 7.8$ W/cm^2.

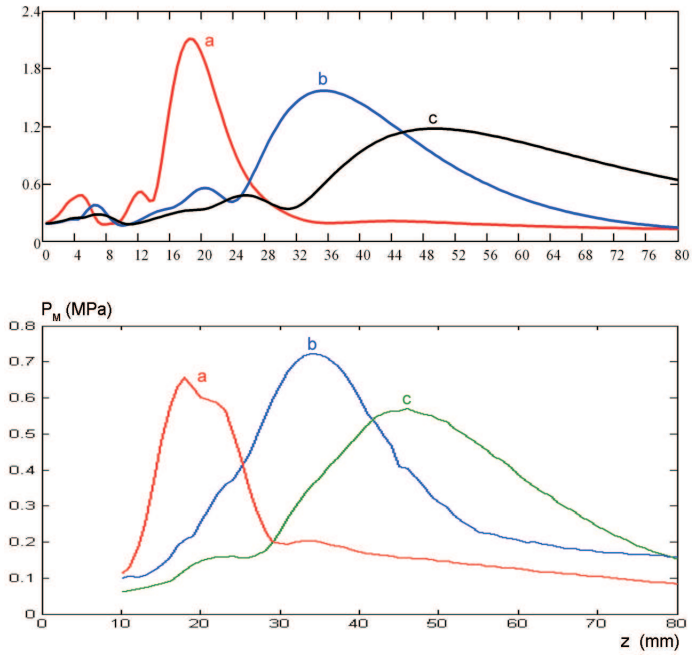

Fig. 4. The acoustic pressure calculated RMS value on axis (top) the and measured peak-to-peak value in MPa (bottom). Three different curves represent focal depths at 20 mm (a), 40 mm (b) and 60 mm (c), respectively.

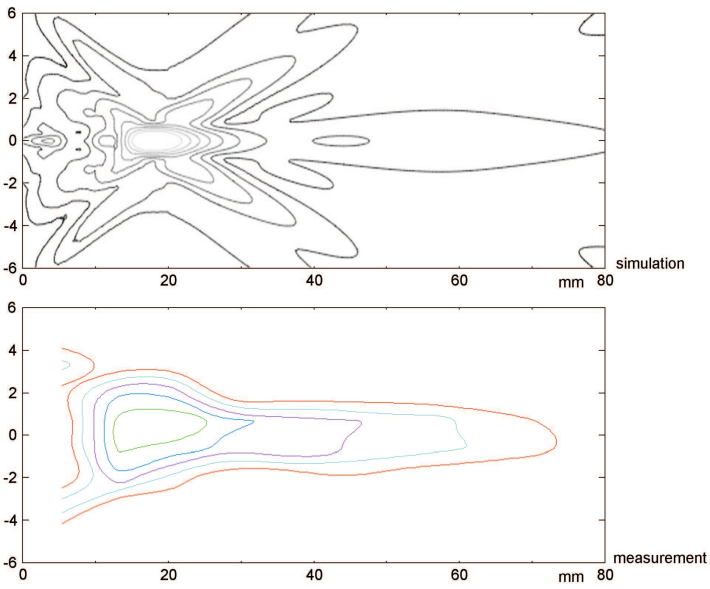

Fig. 5. Two dimensional image of the acoustic fields calculated (top) and measured (bottom) for the annular array transducer focused at 20 mm. Both images present the axial distribution within the 0 and 80 mm range and lateral distribution within ±6 mm off axis range. Isobaric lines are 2 dB steps of the acoustic pressure.

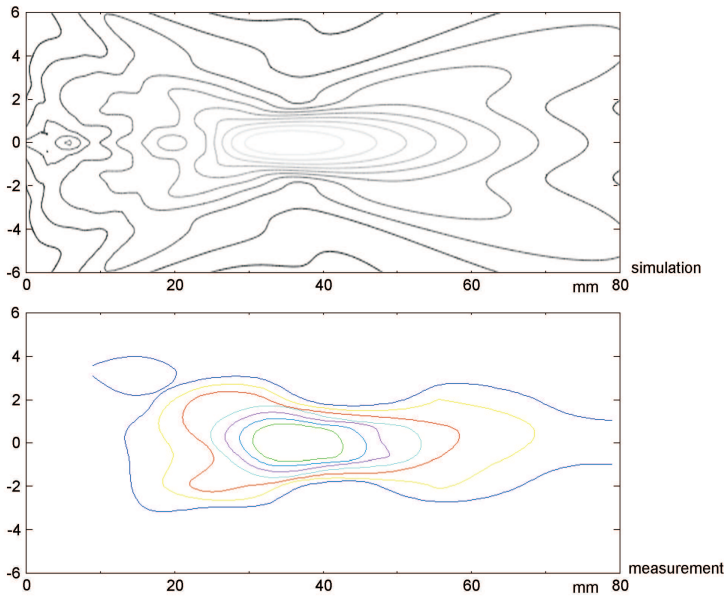

Fig. 6. Two dimensional image of the acoustic fields calculated (top) and measured (bottom) for the annular array transducer focused at 40 mm. Both images present axial distribution within the 0 and 80 mm range and lateral distribution within ±6 mm off axis range. Isobaric lines are 2 dB steps of the acoustic pressure.

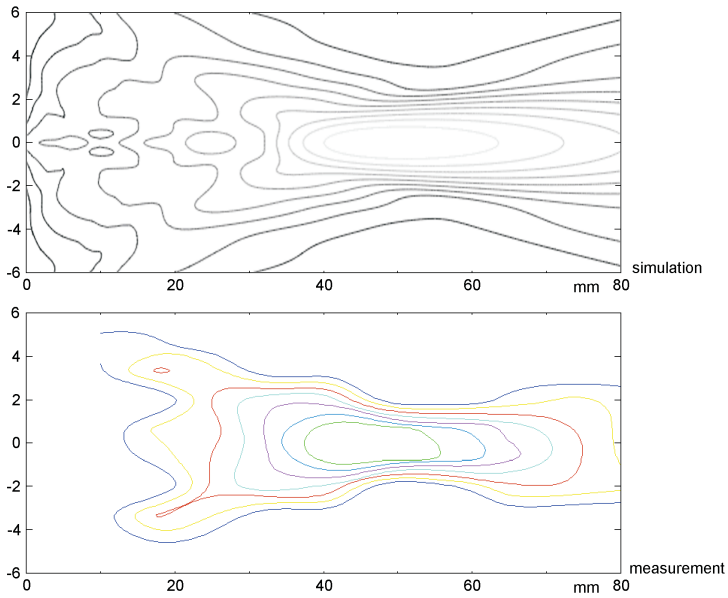

Fig. 7. Two dimensional image of the acoustic fields calculated (top) and measured (bottom) for the annular array transducer focused at 60 mm. Both images present axial distribution within the 0 and 80 mm range and lateral distribution within ±6 mm off axis range. Isobaric lines are 2 dB steps of acoustic pressure.

The measured acoustical power versus amplifier supply voltage is given in Table 1. Also values of the supplied DC power are included.

Table 1. Measured acoustical output power of the transducer PACOUST and electrical transmitter DC supply power PCC versus differential supply voltage VCC.

V_{CC}	±20 V	±22 V	±24 V	±26 V	±28 V	±30 V
P_{CC}	5.6 W	6.6 W	8.2 W	9.1 W	10.4 W	11.7 W
P_{ACOUST}	1.2 W	1.4 W	1.7 W	1.9 W	2.2 W	2.4 W

5. Conclusions

The authors have designed and built a seven element circular array transducer operating at the 2.4 MHz center frequency. Each array element (ring) was excited by a separate power amplifier designed for this project. The final application of this setup was the ultrasonic therapy, the local temperature increase in the healing tissue. The main advantage of the circular array design is the possibility of the focus repositioning and the concentration of ultrasonic beam at a selected depth. Due to FPGA electronics, the focal depth of the transducer is easily programmable by a computer.

For the experiments, three depths were selected: 20, 40 and 60 mm geometrical focus – the places on transducers' axis, where sums of acoustical paths and electronic delays are the same for each element. The physical focus – the place where maximum acoustical pressure exists is closer to the transducer. For the selected delays, it was 19, 35 and 46 mm, respectively. These results were computed and compared to the acoustical field measured in water. Practical results were very close to theory, which proved that the design of the transducer and electronic circuits was correct. Both the focal depth position on axis and lateral width of the focus were equal within the measurement accuracy. The differences are visible only on the shapes of sidelobes at pressures below 10 dB compared to the focal point and are negligible in heating applications of the transducer. These phenomena caused probably by the different admitances of each element. The peak acoustical pressure measured at 40 mm was higher than at 20 mm due to water nonlinearity.

The transducer with matched transmitter was able to generate 2.4 W of acoustical power, which is sufficient for the low intensity focused ultrasound (LIFU) medical applications. In the future work, the system will be used for controlled tissue heating and the temperature rise. The temperature distribution will be compared to the fixed focus transducer.

Acknowledgments

This work was supported by the project POIG.01.03.01-14–012/08-00 co-financed by the European Regional Development Fund under the Innovative

Economy Operational Programme. The project is governed by the Ministry of Science and Higher Education, Poland.

Preliminary results of this study were presented at the Open Seminar on Acoustics, Gliwice, September 20–24, 2010.

References

1. Arditi M., Taylor W. *et al.* (1982), *An annular array system for high resolution breast echography*, Ultrasonic Imaging, **4**, 1, 1–31.
2. Gambin B., Kujawska T. *et al.* (2009), *Temperature Fields Induced by Low Power Focused Ultrasound in Soft Tissues During Gene Therapy. Numerical Predictions and Experimental Results*, Archives of Acoustics, **34**, 4, 445–459.
3. ter Haar G. (1999), *Therapeutic ultrasound*, Eur. J. Ultrasound, **9**, 1, 3–9.
4. ter Haar G. (2008), *The Resurgence of Therapeutic ultrasound – A 21st Century Phenomenon*, Ultrasonics, **48**, 4, 233.
5. Shuto J., Ichimiya I., Suzuki M. (2006), *Effects of low-intensity focused ultrasound on the mouse submandibular gland*, Ultrasound Med. Biol., **32**, 4, 587–594.
6. Wójcik L., Kujawska T., Nowicki A. (2008), *Pulsed nonlinear acoustic fields from clinically relevant sources: numerical calculations and experiments results*, Archives of Acoustics, **33**, 4, 565–571.
7. Wójcik J., Filipczyński L., Kujawska T. (1999), *Temperature elevation computed for three-layer and four-layer obstetrical tissue models in nonlinear and linear propagation cases*, Ultrasound Med. Biol., **25**, 5, 259–267.